Large-scale cortical connectivity dynamics of intrinsic neural oscillations support adaptive listening behavior

Mohsen Alavash*, Sarah Tune, Jonas Obleser*

Department of Psychology, University of Lübeck, 23562 Lübeck, Germany

Center for Brain, Behavior, and Metabolism, University of Lübeck, 23562 Lübeck, Germany

Abstract

In multi-talker situations individuals adapt behaviorally to the listening challenge mostly with ease, but how do brain neural networks shape this adaptation? We here establish a long-sought link between large-scale neural communications in electrophysiology and behavioral success in the control of attention in challenging listening situations. In an age-varying sample of N = 154 individuals, we find that connectivity between intrinsic neural oscillations extracted from source-reconstructed electroencephalography is top-down regulated during a challenging dual-talker listening task. These dynamics emerge as spatially organized modulations in power-envelope correlations of alpha and low-beta neural oscillations during ~2 seconds intervals most critical for listening behavior relative to resting-state baseline. First, left frontoparietal low-beta connectivity (16–24 Hz) increased during anticipation and processing of spatial-attention cue before speech presentation. Second, posterior alpha connectivity (7–11 Hz) decreased during comprehension of competing speech, particularly around target-word presentation. Connectivity dynamics of these networks were predictive of individual differences in the speed and accuracy of target-word identification, respectively, but proved unconfounded by changes in neural oscillatory activity strength. Successful adaptation to a listening challenge thus latches onto two distinct yet complementary neural systems: a beta-tuned frontoparietal network enabling the flexible adaptation to attentive listening state and an alpha-tuned posterior network supporting attention to speech.

Keywords attentive listening; individual differences, large-scale cortical connectivity; alpha/beta oscillations; source EEG

Corresponding author Mohsen Alavash, Jonas Obleser; Maria-Goeppert-Str. 9a, 23562 Lübeck, Germany mohsen.alavash@uni-luebeck.de; jonas.obleser@uni-luebeck.de

Significance Statement

Attending to relevant information during listening is key to human communication. How does this adaptive behavior rely upon neural communications? We here follow up on the long-standing conjecture that, large-scale brain network dynamics constrain our successful adaptation to cognitive challenges. We provide evidence in support of two intrinsic, frequency-specific neural networks that underlie distinct behavioral aspects of successful listening: a beta-tuned frontoparietal network enabling the flexible adaptation to attentive listening state, and an alpha-tuned posterior cortical network supporting attention to speech. These findings shed light on how large-scale neural communication dynamics underlie attentive listening and open new opportunities for brain network-based intervention in hearing loss and its neurocognitive consequences.

Introduction

Noisy, multi-talker listening situations make everyday communication challenging: how to focus only on what we want to hear? Behavioral adaptation to a listening challenge is often facilitated by listening cues (e.g., spatial location or semantic context) and requires individual cognitive ability to control attention (Shinn-Cunningham and Best, 2008; Peelle, 2017). How do a listener's brain networks shape this behavioral adaptation? Addressing this question is essential to neurorehabilitation of the hearing impaired or to the advancement of aided hearing (Lin et al., 2013; Deal et al., 2017).

Our recent study provided a large-scale brain network account of successful listening (Alavash et al., 2019). Using functional magnetic resonance imaging (fMRI), we measured participants' brain hemodynamic responses during task-free resting state and a challenging speech comprehension task. We were able to explain individual adaptation to the listening challenge by reconfiguration of an auditory-control brain network towards increased modular segregation during attentive listening. Knowing the indirect relationship between brain hemodynamics and neural oscillatory dynamics (Laufs et al., 2003; Mantini et al., 2007; Hipp and Siegel, 2015), our study posed an important underexplored question: whether and how network interactions between intrinsic neural oscillations change to support behavioral adaptation to a listening challenge?

Electro-/Magnetoencephalography (E/MEG) studies on attentive listening provide ample evidence supporting the role of neural oscillatory activity within the alpha band (~8–12 Hz) in top-down attentional control over incoming auditory streams (Foxe and Snyder, 2011). Specifically, attentional modulation of alpha-band power has been reported extensively when listeners selectively attend to one of two (or more) concurrent sounds (Banerjee et al., 2011; Müller and Weisz, 2012; Weisz et al., 2014; Wöstmann et al., 2016; Dai et al., 2018; Tune et al., 2018; Wöstmann et al., 2019). These findings have been often interpreted in the light of the widely recognized inhibitory role of alpha oscillations as top-down modulation of cortical excitability (Jensen and Mazaheri, 2010; Van Diepen et al., 2019).

However, these studies have usually investigated how selective attention modulates the power of neural activity and assume cortical alpha rhythms in temporal or parietal regions to underlie these dynamics (Billig et al., 2019). Studies on visual-spatial attention have provided initial evidence on how functional or structural connectivity between distant cortical regions mediate such top-down attentional modulations in alpha or other frequency bands (Marshall et al., 2015a; Bonnefond et al., 2017; Popov et al., 2017; D'Andrea et al., 2018). Nevertheless, we do not know yet whether and how

attentive listening relies on intrinsic neural oscillations acting in concert across distributed cortical networks.

Large-scale neural interactions at slow time scales (<0.1 Hz) have been suggested as a proxy of functional coordination between distant brain areas. Specifically, power-envelope fluctuations of ongoing alpha- and beta-band oscillations (~13–30 Hz) exhibit this characteristic, and their intrinsic co-modulations over time correlate with co-variation of brain hemodynamic signals during resting state (Mantini et al., 2007; Brookes et al., 2011; Hipp et al., 2012; Hipp and Siegel, 2015). Accordingly, these neural dynamics have been proposed as one network mechanism whereby distant cortical regions functionally coordinate their activity to participate in a task (Palva and Palva, 2012; Siegel et al., 2012; Engel et al., 2013). How intrinsic neural oscillations regulate their power-envelope coupling in adaptation to attentive listening is unknown.

Moreover, it is not yet fully understood why listeners exhibit substantial inter-individual variability in successful adaptation to a listening challenge (Mattys et al., 2012; Tamati et al., 2013). This variability seems to arise from differences in sensory coding fidelity, from differences in the ability to use cognitive resources, or from a combination of both (Shinn-Cunningham, 2017; Dai et al., 2018). To what degree this inter-individual variability relates to listeners' ability to top-down regulate amplitude-coupling between neural oscillations is unknown.

The present large-sample EEG study regards the neocortical systems involved in attentive listening as an assembly of dynamic large-scale networks of ongoing neural oscillations. Building on our previous work on brain hemodynamic networks during the same experimental paradigm (Alavash et al., 2019), we treat the resting-state network makeup of intrinsic neural oscillations as their putative task network at its "idling" baseline. We predict neural oscillations to regulate their amplitude-coupling and/or reconfigure their network in adaptation to attentive listening. We expect these changes to manifest in the alpha–beta frequency range and leverage the degree of these changes as a proxy of individuals' successful adaptation to a listening challenge.

Results

We recorded 64-channel scalp EEG from a large, age-varying sample of healthy middle-aged and older adults (N = 154; age range = 39–80 yrs, median age = 61 yrs; 62 males). This includes thirty individuals who have had participated in our previous fMRI study and performed the same listening task (Alavash et al., 2019). All participants were recruited as part of an on-going large-scale longitudinal study (see *Data collection* for details). Each participant completed a five-minute eyes-open resting state measurement and one-hour of the listening task. The listening task was identical to the one used in (Alavash et al., 2019) and can be viewed as a linguistic Posner paradigm (Figure 1).

In brief, participants were dichotically presented with two five-word sentences and were instructed to identify the final word (i.e., target) of one of these two sentences. To probe individual use of auditory spatial attention and semantic prediction when confronted with a listening challenge, sentence presentation was preceded by two visual cues. First, a spatial-attention cue either indicated the to-be-attended side, thus invoking selective attention, or it was uninformative, thus invoking divided attention. The second cue informed about the semantic category of both final words either very generally or more specifically, allowing for more-or-less precise semantic prediction of the upcoming target word.

We source-localized narrow-band EEG signals recorded during rest and task, and following leakage correction, estimated power-envelope correlations between all pairs of cortical regions

defined according to a symmetric whole-brain parcellation template (Figure S1). We asked whether and how amplitude-coupling between intrinsic neural oscillations changes throughout the listening task as compared to resting state. Importantly, using (generalized) linear mixed-effects models, we examined the influence of listening cues and frequency-specific network dynamics on single-trial listening performance, accounting for individuals' age, hearing thresholds, and neural oscillatory power.

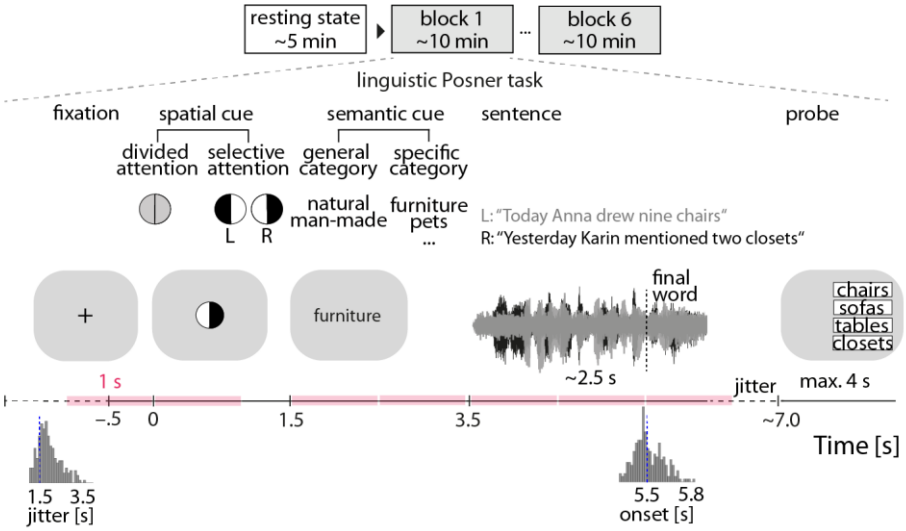

Figure 1. Experimental procedure and the listening task. EEG of N = 154 participants was recorded during a 5-min eyes-open resting state and six blocks of a linguistic Posner task with concurrent speech (Alavash et al., 2019). Participants listened to two competing, dichotically presented sentences. Each trial started with the visual presentation of a spatial cue. An informative cue provided information about the side (left ear vs. right ear) of the to-be-probed final word. An uninformative cue did not provide information about the side of the to-be-probed final word. A semantic cue was visually presented indicating a general or a specific semantic category for both final words. The two sentences were presented dichotically along with a visual fixation cross. At the end of each trial a visual response array appeared on the side of the probed ear with four word-choices, asking participants to identify the final word of the sentence presented to the respective ear. To capture amplitude-coupling between frequency-specific neural oscillations throughout the listening task, power-envelope correlations between narrow-band EEG sources were estimated within one-second time windows of interest (colored intervals) and compared with resting state connectivity at the same frequency

Informative cues improve listening success

The analysis of listening performance using linear mixed-effects models revealed an overall behavioral benefit from more informative cues. The behavioral effects reported below are in good agreement with the results obtained before using the same task in fMRI (Alavash et al., 2019) Specifically, listeners performed more accurately and faster under selective attention as compared to divided attention (accuracy: odds ratio (OR) = 3.4, $p < 0.001$; response speed: $\beta = 0.57$, $p < 0.001$; Figure 2A and B, top row of scatter plots). Moreover, listeners performed faster when they were cued to the specific semantic category of the final word as compared to a general category ($\beta = 0.12$, $p < 0.001$; Figure 2B, second scatter plot). We did not find evidence for any interactive effects of the two listening cues in predicting accuracy (OR = 1.3, $p = 0.15$) or response speed ($\beta = 0.09$, $p = 0.29$).

As expected, the older a listener the worse the performance (main effect of age; accuracy: OR = 0.78, $p < 0.01$; response speed: $\beta = -0.15$, $p<0.001$). Furthermore, as to be predicted from the right-ear advantage for linguistic materials (Kimura, 1961; Broadbent and Gregory, 1964), listeners were more accurate and faster when probed on the right compared to the left ear (main effect of probe

on accuracy: OR = 1.25, p < 0.01; response speed: β = 0.09, p<0.001). In addition, the number of blocks participants completed (six in total) had a main effect on task performance (accuracy: OR = 1.28, p < 0.001; response speed: β = 0.11, p<0.001) indicating that individuals' listening performance improved over task blocks (see Table S1 and S2 for all model terms and estimates).

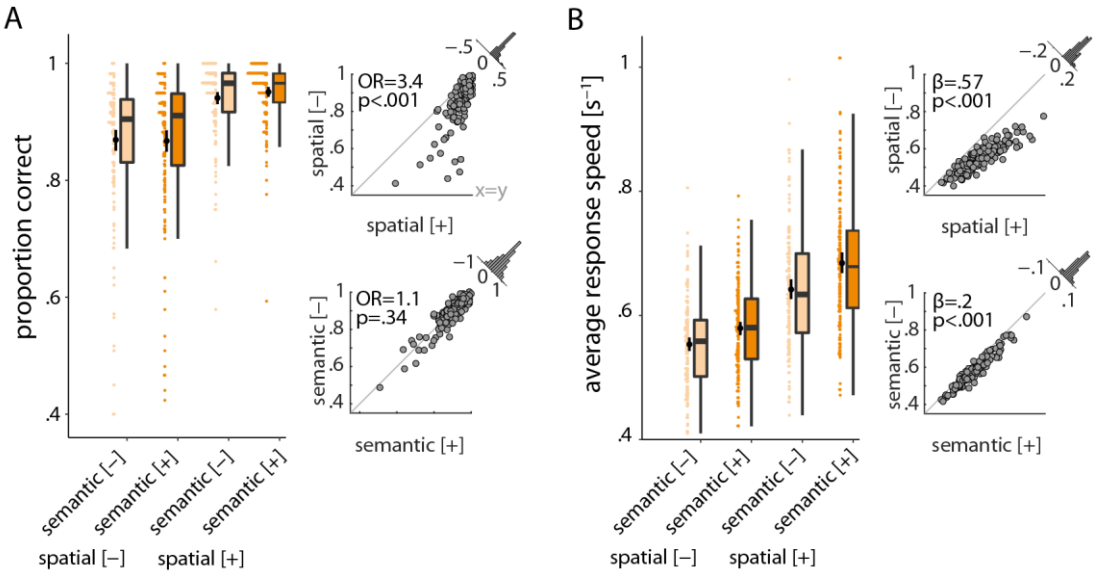

Figure 2. Individual behavioral benefit from informative listening cues. **(A)** Proportion of correct final word identifications averaged over trials per cue condition **(B)** The same as (A) but for average response speed. *Box plots*: Colored data points represent trial-averaged performance scores of N = 154 individuals per cue-cue combination. Black bars show mean ± bootstrapped 95% CI. *Scatter plots*: Individual cue benefits shown separately for each cue and performance score. Black data points represent individuals' trial-averaged scores under informative [+] and uninformative [–] cue conditions. Gray diagonal corresponds to 45-degree line. Histograms show the distribution of the cue benefit (informative minus uninformative) across all participants. *OR*: Odds ratio parameter estimate resulting from generalized linear mixed-effects models; *β*: slope parameter estimate resulting from general linear mixed-effects models

Spectral and spatial profile of power-envelope correlations under rest and listening

Central to the present study, we asked whether and how amplitude-coupling between intrinsic neural oscillations changes as individuals engage in attentive listening. To answer this question, we first investigated the spectral and spatial profile of power-envelope correlations estimated under rest and the listening task.

In line with previous studies (e.g., Hipp et al., 2012; Hipp and Siegel, 2015; Siems et al., 2016), power-envelope correlations were strongest in the alpha to low-beta frequency range (7–24 Hz) and proved reliable in this range under both rest and task conditions (between-subject analysis; Figure S2A-C). In addition, across thirty individuals who had participated in both the present EEG study and our previous fMRI study (Alavash et al., 2019), EEG mean connectivity showed consistently positive correlations with fMRI mean connectivity within the same frequency range (Figure S2D and E).

Accordingly, we focused our main analysis on three frequency bands within 7–24 Hz, namely α_1(7–11 Hz), α_2(11–14 Hz), and β_1(16–24 Hz). The main analysis began by investigating group-average whole-brain connectivity per frequency band under rest and listening task.

As shown in Figure 3, rest and task connectivity showed overall similar spatial profiles across cortex. More precisely, power-envelope correlations in both α_1 and α_2 range were strongest within

and between bilateral occipital and temporal nodes, but also across occipitoparietal as well as temporoparietal nodes under rest or listening task (Figure 3, first column; see Figure S4 for α_2 connectivity). In contrast, frontal nodes displayed relatively sparse connectivity. Power-envelope correlations in β_1 frequency range displayed similar spatial pattern, but with the left-hemispheric connections showing relatively stronger connectivity under listening task as compared to rest (Figure 3, second column).

To evaluate connectivity strength of each cortical node, we used a simple graph-theoretical measure—namely nodal connectivity—defined as the sum of each node's connection weights. This analysis revealed a long-tailed distribution of nodal connectivity across cortex, where nodes with highest connectivity strength localized to occipital and temporal regions in both the alpha and low-beta frequency range (Figure 3, cortical maps).

We next investigated the network topology of these connectivity profiles. Specifically, we asked whether these cortical correlation structures exhibit modular organization. In our previous fMRI study hemodynamic brain networks had displayed modular organization under both rest and the same listening task (Alavash et al., 2019). Qualitatively, in a modular network one would expect groups of nodes which are relatively *densely* intra-connected, but relatively *sparsely* inter-connected. We thus predicted EEG source connectivity to be also functionally decomposable into network modules.

However, we found that neither alpha nor low-beta connectivity displayed modular organization under rest or listening: the module detection algorithm revealed only unevenly dense modules and relatively small modularity indices (Figure S3). Collectively, these results illustrate that power-envelope correlations in the alpha and low-beta frequency range were predominantly present across sensory and parietal association regions. However, amplitude-coupling between these regions did not topologically segregate to exhibit a modular organization.

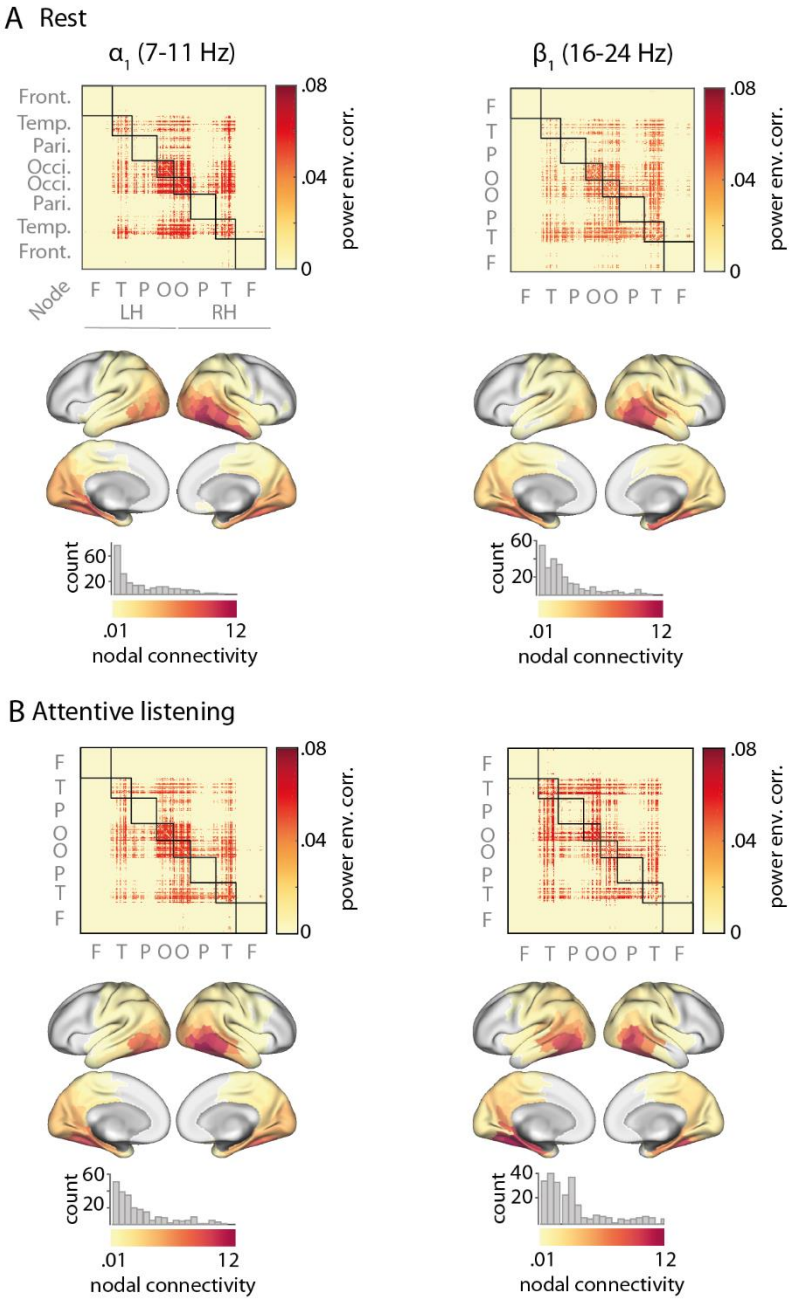

Figure 3. Connectivity maps of α/β oscillations under rest and attentive listening. **(A)** For each frequency band, power-envelope correlations between EEG sources were estimated using 5-min eyes-open resting state data **(B)** The same procedure as in (A) was applied to task data after concatenating whole-trial signals across 30 random trials of each block (5-min data in total), and then averaging the correlation matrices across all six blocks of task. Connectivity maps were averaged across N = 154 individuals and thresholded at 10% of network density. Nodes having zero connectivity are masked in grey. Histograms illustrate distribution of nodal connectivity with high-connectivity nodes overlapping with occipital and posterior temporal regions. Note that in this analysis task connectivity is not specific to a particular time window within trials or cue condition, and thus illustrate the overall spatial profile of α/β connectivity under listening task. Nodes correspond to cortical parcels as in (Glasser et al., 2016) and are identified according to their anatomical labels. *LH*: left hemisphere; *RH*: right hemisphere.

Hyperconnectivity of frontoparietal β oscillations in anticipation of and during spatial cueing

To investigate whether and how power-envelope correlations between neural oscillations change throughout the listening task, we leveraged the high temporal resolution of EEG and defined 1-s time windows of interest throughout the entire trial (Figure 1, colored intervals). This allowed us to estimate connectivity for each frequency band and time window by concatenating windowed narrow-band signals across all 240 trials (equivalently, 4-min data). We then compared the results with 4-min resting state connectivity at the same frequency band by subtracting task and rest connectivity matrices.

During anticipation of the spatial-attention cue (−1–0 s), β_1 connectivity showed an increase relative to resting state (Figure 4A, left panel, first connectivity matrix). This hyperconnectivity was observed most prominently within the left temporal cortex, as well as between frontal, temporal, and parietal regions. Using permutation tests to compare nodal connectivity between rest and task, we found that β_1 connectivity of mainly left prefrontal and parietal nodes was increased during anticipation of the spatial cue relative to rest ($0.29 < \text{Cohen's } d < 0.46$, $p < 0.01$, FDR-corrected for multiple comparisons across nodes; significant nodes are outlined in black in Figure 4A, first panel, first cortical maps). In contrast, alpha connectivity during this period was not significantly different from resting state (Figure S5A)

Next, we focused on 1-s time windows capturing the presentation of each listening cue. During the spatial cue presentation (0–1 s), β_1 connectivity of left prefrontal and parietal regions remained significantly higher than rest ($0.29 < d < 0.44$, $p < 0.01$; Figure 4A, first pane, second connectivity matrix; see Figure S4 for non-differential connectivity matrices). During the same period, alpha-band connectivity showed a relative decrease which was only significant in α_1 range and over a few parietal nodes (Figure S5B, first panel). During the semantic cue period (1.5–2.5 s) power-envelope correlations were not significantly different from resting state in neither the alpha nor in low-beta range (Figure S5C).

To assess the degree and direction to which each listener showed β_1 hyperconnectivity during presentation of the spatial cue, we averaged nodal connectivity across frontoparietal regions per individual. We then statistically compared individuals' mean connectivity values between rest and task using a permutation test. In accordance with the results at the nodal level, mean frontoparietal β_1 connectivity was significantly higher than rest during presentation of the spatial cue ($d = 0.6$, $p < 0.01$; Figure 4B, first panel).

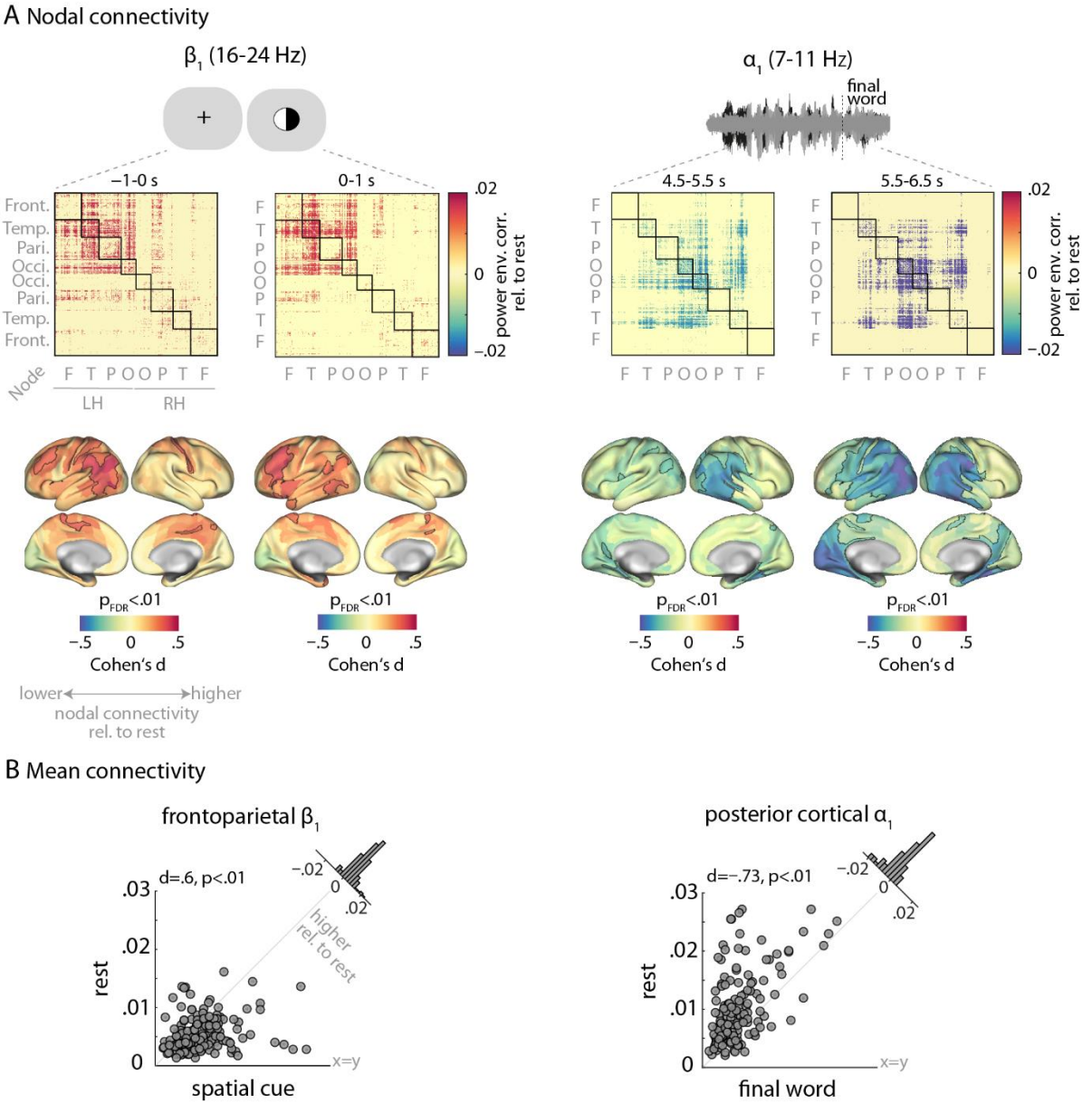

Figure 4. Cortical connectivity dynamics of α/β oscillations during the listening task. **(A)** To assess whether and how intrinsic alpha and low-beta oscillations regulate their cortical connectivity during adaptive listening, connectivity difference maps (i.e., task minus rest) were calculated per frequency band. Task connectivity was extracted by concatenating one-second windowed signals across all 240 trials (4-min data). In anticipation of and during the spatial cue presentation β_1 connectivity was increased relative to its intrinsic connectivity mainly within the left hemisphere (first panel). This hyperconnectivity was significant across frontoparietal regions (brain surfaces; significant nodes are outlined in black). The same analysis revealed a significant alpha hypoconnectivity during final-word presentation (second panel). **(B)** To assess the degree and direction of change in connectivity per individual listener, nodal connectivity was averaged across significant nodes and compared between rest and task using permutation tests. Data points represent individuals' mean connectivity (N = 154). Gray diagonal corresponds to 45-degree line. Histograms show the distribution of the connectivity change (task minus rest) across all participants.

Hypoconnectivity of posterior cortical α oscillations during listening to speech

During the listening task, participants were asked to identify the final word of one of two concurrent sentences. The sentences were presented after the two listening cues, and on average had a duration of around 2.5 s (Figure 1). Accordingly, we divided the sentence presentation period (3.5–6.5 s) into three consecutive one-second intervals and estimated connectivity for each frequency band and time window. This analysis revealed a gradual decrease in alpha connectivity across posterior parts of the brain during sentence presentation relative to resting state.

Specifically, during sentence presentation (3.5–6.5 s), α_1 connectivity within and between bilateral occipital regions was decreased relative to resting state, particularly so during the interval around the final-word presentation (Figure 4A, second panel). This hypoconnectivity was also observable between occipital and temporo-parietal regions and in the α_2 band (Figure S6). In contrast, β_1 connectivity during sentence presentation was not significantly different from resting state (Figure S6A-C, third column).

When tested at the nodal level, the alpha-band hypoconnectivity overlapped with posterior temporal cortices as well as occipital and parietal regions ($-0.5 < d < -0.23$, $p < 0.01$; nodes outlined in black in Figure 4A, second panel, cortical maps). Notably, when averaged across the posterior cortical nodes, individuals showed consistently lower mean connectivity during final-word presentation relative to rest (Figure 4B, second panel).

Connectivity dynamics of intrinsic α/β oscillations predict individual listening behavior

The results illustrated above can be outlined as spatiotemporal modulations in alpha and low-beta connectivity throughout the listening task relative to resting state. As Figure 4B shows, listeners clearly showed inter-individual variability in the degree and direction of these connectivity dynamics. Thus, we next investigated whether these variabilities could account for inter-individual variability in listening performance (Figure 2).

To this end, we tested the direct and interactive effects of individual mean connectivity during resting-state and during each listening task interval (i.e., spatial-cue or final-word periods) on individuals' accuracy or response speed. These brain-behavior relationships were tested in separate models per alpha or low-beta band. In each model, brain regressors were the mean connectivity of the posterior alpha or frontoparietal low-beta networks on individual-level, respectively. These are the same linear mixed-effects models based on which the beneficial effects of informative listening cues on behavioral performance was reported earlier.

Figure 5 illustrates the main brain-behavior results. First, we found that frontoparietal β_1 connectivity during spatial cueing predicted listeners' response speed in the ensuing final-word identification, but only in those individuals whose resting-state β_1 connectivity of the same network was lower than average (by half-SD or more). Statistically, this surfaced as a significant interaction between mean resting-state frontoparietal β_1 connectivity and mean connectivity of the same network during spatial-cue presentation in predicting listeners' response speed ($\beta = 0.019$, $p < 0.01$; Figure 5A; see Table S6 for details). This indicated that, among individuals with lower than average resting-state frontoparietal β_1 connectivity (N = 41), increased connectivity during spatial cueing was associated with slower responses during final-word identification ($\beta = -0.034$, $p < 0.01$; Figure 5A, first panel).

Second, mean posterior α_1 resting-state connectivity and mean connectivity of the same network during final-word presentation jointly predicted a listener's accuracy (OR = .94, p = 0.04;

Figure 5B; see Table S1 for details). This interaction indicated that the behavioral relevance of α_1 hypoconnectivity during final-word identification was conditional on individuals' resting-state α_1 connectivity: for listeners with an intrinsic α_1 connectivity higher than average (by half-SD or more; N = 45), there was a significant negative correlation between α_1 connectivity during final-word presentation and overall word identification accuracy (OR = 0.88, p = 0.04, Figure 5B, third panel).

Additionally, in separate models we tested the above interactions using connectivity during anticipation of the spatial cue (i.e., −1-0 s fixation) as baseline instead of resting state connectivity. Notably, the β_1 interaction in predicting listeners' response speed was absent (β = 0.001, p = 0.89), as was the α_1 interaction in predicting listeners' accuracy (OR = 0.98, p = 0.5).

We also investigated the reliability and robustness of the brain-behavior findings using 5-fold cross-validation and examined the strength and significance of the model's parameter estimate when random subsets of data were used. To assess the likelihood that the observed data are better explained by the model including the respective interaction terms, we also calculated the Bayes factor (BF). By convention, a log-BF of 1 begins to lend support to the H1(Dienes, 2014).

The cross-validation results obtained for the model predicting response speed from frontoparietal β_1 connectivity dynamics were well in line with those obtained from the full sample (Figure S10A): For all five model iterations, the β estimate of the interaction term was significantly larger than zero, and the log-BF estimate was larger than 1 in three model iterations. For the model predicting accuracy from posterior α_1 connectivity dynamics, for four model iterations the odds ratio was significantly smaller than 1, indicating a negative correlation, and the log-BF estimate was larger than 1 in one model iteration.

In support of the behavioral relevance of alpha and low-beta connectivity we also found their significant interactions with task-block number in predicting individuals' accuracy (α_1: OR = 0.91, p < 0.01; α_2: OR = 0.92, p < 0.01; β_1: OR = 0.95, p = 0.02,) or response speed (α_1: β = −0.021, p < 0.001; α_2: β = −0.032, p < 0.001; see Table S1-5 for details). These interactions indicated that (1) those listeners with lower posterior alpha connectivity during final-word presentation showed improved behavioral performance over six blocks of task and (2) listeners with lower β_1 connectivity during presentation of the spatial cue showed improved accuracy over task blocks.

We did not find any evidence for the behavioral relevance of the α_2 band connectivity dynamics, i.e., its interaction with resting state connectivity (see Table S3-4 for details). The interactions between mean connectivity or neural oscillatory power with the listening cues in predicting behavior were also not significant in neither of the frequency bands.

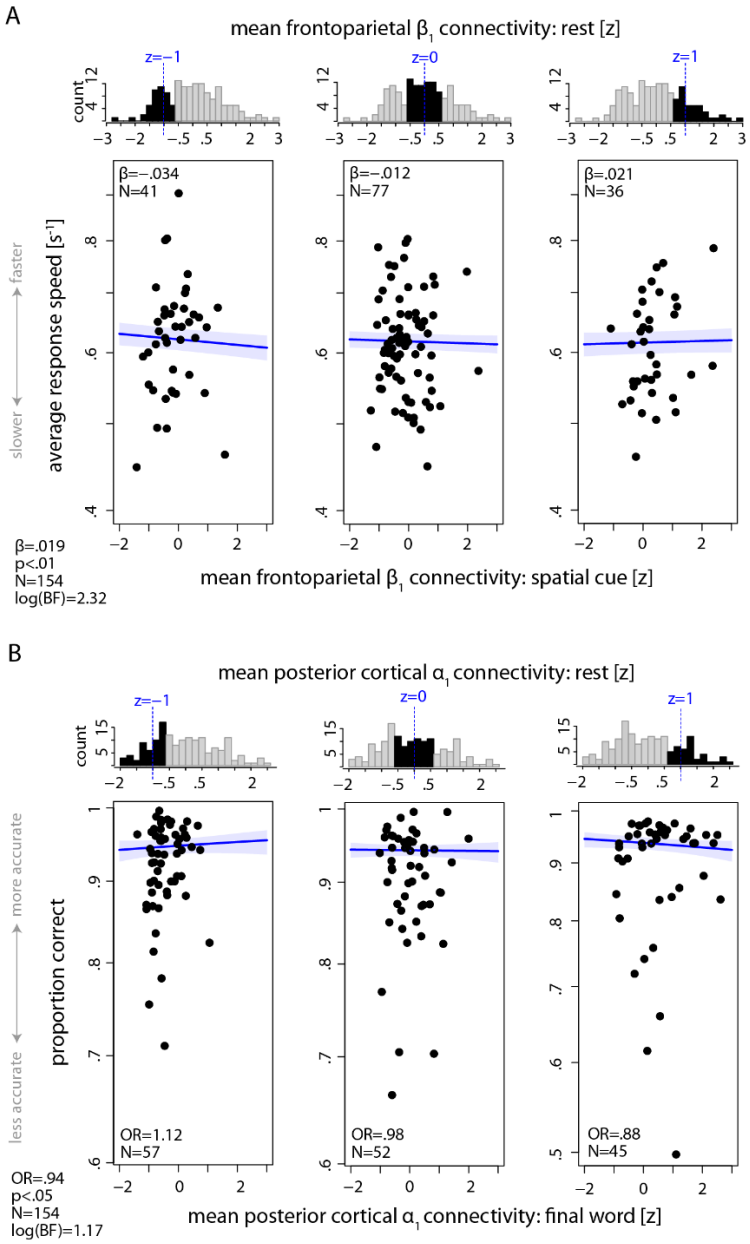

Figure 5. Prediction of individual listening behavior from α/β connectivity dynamics. **(A)** Interaction between mean frontoparietal β_1 connectivity derived from resting state and connectivity of the same network during spatial cue presentation predicted how fast listeners identified the final word in the ensuing sentence presentation (β = 0.019, p < 0.01, log-BF = 2.32). For visualization purpose only, individuals were grouped according to their standardized mean frontoparietal β_1 resting state connectivity. Each scatter plot corresponds to one group of individuals. Distribution of mean connectivity for each group is highlighted in black within the top histograms. Black data points represent the same individuals' trial-average response speed regressed on their standardized mean frontoparietal $\beta_1$connectivity during spatial cueing. Solid blue lines indicate linear regression fit to the data when β_1 resting state connectivity held constant at the group mean (dashed blue line in histograms). **(B)** Interaction between mean posterior α_1 connectivity derived from resting state and connectivity of the same network during final word presentation predicted listeners' word identification accuracy (OR = 0.94, p < 0.05, log-BF = 1.17). Data visualization is the same as in (A), but here the grouping variable is mean posterior α_1 resting state connectivity and the predictor is the mean connectivity of the same network during final word period. Individuals' age and hearing thresholds have been accounted for in the models. Shaded area shows two-sided parametric 95% CI. *β*: Slope parameter estimates from linear mixed-effects model. *OR*: Odds ratio parameter estimates from generalized linear mixed-effects models. *BF*: Bayes factor.

Control analysis: are α/β connectivity effects confounded by changes in activation?

A recurring theme in studying neural interactions is to what extent connectivity estimates are mere reflection of neural activation (Pesaran et al., 2018; Tewarie et al., 2018). As an extreme scenario, connectivity between two regions could be purely driven by instantaneous changes in neural activity (or signal-to-noise ratio) of each region and not their genuine functional connectivity. We therefore conducted a set of control analyses to assess the degree to which the dynamics of power-envelop correlations found here could be mere reflection of changes in alpha or low-beta power.

As illustrated in Figure S7, grand-average power of narrow-band EEG signals during anticipation of the spatial cue was higher than baseline within 7–24 Hz, and it was decreased in response to both listening cues. This modulation was similarly observed during sentence presentation and appeared stronger during final-word presentation. For the final-word period, we also quantified hemispheric lateralization of alpha-band activity (7–14 Hz) based on selective-attention trials and using the so-called attentional modulation index (AMI); AMI = ($\alpha\text{-power}_{\text{attendL}} - \alpha\text{-power}_{\text{attendR}}$) / ($\alpha\text{-power}_{\text{attendL}} + \alpha\text{-power}_{\text{attendR}}$). As expected, source alpha power was lower over the hemisphere contralateral to the side of attention (Figure S7C). At first glance, these changes in power appear similar to the power-envelope correlation dynamics reported earlier. To directly investigate this, we conducted the following analyses.

First, for each cortical node, we tested the correlation between nodal connectivity and mean nodal power (dB) during task across participants. During spatial cue period and within β_1 band this correlation was mainly positive across cortex and was significant over a few occipital nodes (Spearman's $\rho = 0.3$, $p < 0.01$; Figure S8A, first panel). However, this relationship and the overall pattern of nodal correlations did not resemble the mainly left-hemispheric frontoparietal β_1 hyperconnectivity (Figure 4A, first panel). Moreover, during final-word presentation, the correlation between mean alpha power (dB) and nodal connectivity showed both positive and negative trends across cortex which did not reach significance level ($-0.25 < \rho < 0.25$, $p > 0.1$; Figure S8A, last two panels, cf. Figure 4A, second panel). When these correlations were tested using mean connectivity and power averaged across frontoparietal or posterior nodes, there was only a positive trend for the correlation between mean frontoparietal β_1 connectivity and power during spatial-cue presentation ($\rho = 0.15$, $p = 0.07$; Figure S8B).

Second, on selective-attention trials and during final-word presentation alpha activity clearly showed a lateralized modulation depending on whether participants attended to left or right ear (Figure S7C). We investigated whether connectivity showed a similar lateralization. Precluding the here observed neural connectivity from being confounded by neural activity level, power-envelope correlations were not influenced by attentional-cue conditions (i.e., left vs. right or selective vs. divided) in neither of the trial intervals or frequency bands (Figure S9).

Third, in our mixed-effects models we included mean neural oscillatory power as a separate regressor, and specifically tested the direct and interactive effects of power on individuals' behavioral performance. We only found a significant main effect of β_1 power during spatial-cue presentation on listeners' response speed ($\beta = -0.029$, $p < 0.01$). Notably, while posterior α_1 connectivity predicted listeners' behavioral accuracy, the data held no evidence for any effect of alpha power on behavior (see Tables S1-4 for details). Additionally, while alpha and low-beta mean connectivity showed significant interactions with task-block number in predicting individuals' behavioral performance (see SI Tables for details), this effect was absent for power.

Lastly, to diminish common covariation in source power due to volume conduction, all time-frequency source estimates in our analyses were orthogonalized across all pairs of cortical nodes

prior to estimating power-envelope correlations (Hipp et al., 2012). This approach eliminates (or at least diminishes considerably), the instantaneous zero- or close to zero-lag correlations between signals (Colclough et al., 2015). Thus, connectivity estimates derived from this procedure are less likely to be contaminated by shared neural activity time-locked to task events.

Discussion

We have shown here how cortical connectivity of intrinsic neural oscillations was regulated in adaptation to a listening challenge. These dynamics were found as spatially organized modulations in power-envelope correlations of alpha and low-beta oscillations during ~2-s intervals most critical for listening behavior relative to resting-state baseline. First, left frontoparietal low-beta connectivity increased during anticipation and processing of the spatial-attention cue before speech presentation. Second, posterior alpha connectivity decreased during comprehension of speech, particularly in the interval around target-word identification. Importantly, these connectivity dynamics predicted distinct aspects of listeners' behavior, namely response speed and accuracy, respectively.

Frontoparietal β connectivity supports flexible adaptation to attentive listening

The listening task required the individuals to process the spatial cue in order to update the information about the relevance of each sentence on a trial-by-trial basis. Behaviorally, this can be viewed as an adaptation to the current listening state. Neurocognitively, this requires top-down allocation of resources responsible for attentional and task-set control.

In our representative sample, listeners with higher frontoparietal β_1 power during processing of the spatial cue showed slower word-identification. Furthermore, among those listeners with resting-state frontoparietal β_1 connectivity lower than average, connectivity of the same network during processing of the spatial cue was negatively correlated with response speed in the ensuing final-word identification. Taken together, stronger frontoparietal β_1 synchrony during spatial-cue processing was associated with slower responses. Accordingly, the strength of frontoparietal β_1 connectivity likely reflects the neural cost that listeners incurred by flexibly updating and restoring the relevance of each left and right sentence on a trial-by-trial basis.

These results extend and help functionally specify the growing consensus that beta synchrony has a role in top-down control of goal-directed behaviors (Engel and Fries, 2010; Miller and Buschman, 2013; Spitzer and Haegens, 2017). Evidence comes from animal and human studies that demonstrate a functional role of prefrontal beta synchronization in task-state transitions when content information—such as stimulus category, memory item, decision choice, or internalized task rule—need to be endogenously maintained or updated (Buschman et al., 2012; Salazar et al., 2012; Siegel et al., 2015; Miller et al., 2018). Task states as such have been found to coincide with short-lived beta synchrony in frontoparietal areas, for example, during stimulus categorization (Antzoulatos and Miller, 2016; Stanley et al., 2016), working memory retention (Spitzer and Blankenburg, 2011; Spitzer et al., 2014) or accumulation of sensory evidence (Siegel et al., 2011; Kelly and O'Connell, 2015).

Interestingly, these findings have been reported mainly in the lower-beta frequency range (~20 Hz) and often in the absence of stimulation, e.g. during delay periods of memory tasks (Wimmer et al., 2016). It is generally recognized that synchrony of low-beta oscillations is initiated in higher-level control areas and propagates to lower-level sensory areas (Bastos et al., 2012; Bastos et al., 2015). In addition, low-beta oscillations seem to have the optimal neurocomputational properties to prepare and maintain neural assemblies in the absence of external input (Kopell et al., 2011; Lee et al., 2013).

Accordingly, momentary frontoparietal low-beta synchrony has been proposed to represent higher-level abstract task content and goals which "awakes" an endogenous cognitive set to control a range of goal-directed behaviors (Spitzer and Haegens, 2017). This proposal is in line with the view that frontoparietal neurons are multi-functional and distributed across multiple ensembles which can be selectively activated by means of synchronous oscillations to flexibly enable adaptive behaviors (Rigotti et al., 2013; Fusi et al., 2016).

Overall, our finding indicates that left-hemispheric frontoparietal β_1 connectivity acts as a top-down network mechanism to re-activate otherwise silent beta oscillations responsible for preparing cortical circuits involved in attentive listening. The strength of this connectivity may be a neural proxy of a listener's flexibility in using spatial cues to cope with challenging listening situations.

Lower posterior cortical α connectivity supports attention to speech

When participants listened to concurrent sentences and particularly to the task-relevant final word, power-envelope correlation between posterior alpha oscillations was diminished. This finding very likely indicates a cohesive shutdown of the posterior alpha-tuned network to promote the spread of cortical information, thereby facilitating selection and comprehension of speech. We note that, during spatial cue presentation, this hypoconnectivity was only weakly observable suggesting that posterior alpha connectivity is top-down downregulated mainly during overt listening behavior.

Over the last twenty years alpha oscillations have been increasingly recognized as a signature of cortical inhibition (Klimesch et al., 2007; Jensen and Mazaheri, 2010; Mathewson et al., 2011). More precisely, one general view is that alpha oscillations prioritize stimulus processing by inhibiting task-irrelevant and disinhibiting task-relevant cortical areas. More recently, this view has been modified and expanded in a more mechanistic way (Van Diepen et al., 2019). Specifically, it has been suggested that during periods of low alpha-power cortical excitability is sufficiently high to allow continuous processing regardless of alpha phase ('medium-to-high' attentional state). In contrast, when alpha power is high, cortical processing is discontinuous and depends on the phase of alpha rhythm ('rhythmic' attentional state) (Palva and Palva, 2011; Jensen et al., 2014). These mechanisms appear across sensory and motor cortices (Haegens et al., 2011; de Pesters et al., 2016; Popov et al., 2017) and point to the critical role of both power and phase dynamics of alpha oscillations in attentional control (Clayton et al., 2018; Fiebelkorn and Kastner, 2020).

For alpha dynamics as such to be under top-down control a link with brain networks must exist. Indeed, it has been previously suggested that three large-scale cortical networks differentially top-down regulate alpha oscillations (Sadaghiani and Kleinschmidt, 2016). Specifically, while phase synchrony of alpha oscillations has been associated with the frontoparietal network involved in adaptive control (Palva and Palva, 2007; Sadaghiani et al., 2012; Sadaghiani et al., 2018), amplitude modulation of alpha oscillations has been proposed to be under control of cingulo-opercular and dorsal attention networks involved in maintaining tonic alertness and guiding selective attention, respectively (Capotosto et al., 2009; Sadaghiani et al., 2010; Marshall et al., 2015b).

Overall, hypoconnectivity of posterior alpha oscillations is likely a manifestation of a broader attentional network process acting on excitability or engagement of sensory channels through their coherent release of inhibition. Our finding thus extends previously proposed inhibitory role of alpha oscillatory activity in attention and suggests that individual attentive listening behavior hinges on both intrinsic posterior alpha amplitude-coupling and its downregulation during selection and comprehension of speech.

Network dynamics of the attentive listening brain: Current state and future directions

Our previous fMRI experiment (Alavash et al., 2019) and the present study take a network neuroscience approach to unravel cortical underpinning of successful adaptation to a listening challenge. The fMRI study suggests that this adaptation is supported by topological reconfiguration of auditory, ventral attention, and cingulo-opercular modules. Our main finding was that functional segregation of this auditory-control network relative to its resting-state baseline predicted individuals' listening behavior. In the present study we found that this adaptation is supported by top-down regulation of connectivity between alpha and low-beta neural oscillations during intervals most critical to listening behavior. Our key finding is that connectivity between frontoparietal low-beta oscillations and posterior alpha oscillations relative to their resting-state baseline is predictive of distinct aspects of individuals' listening behavior. Thus, both studies share a common thread: dynamics of large-scale cortical networks retain the information that could predict trait-like individual differences in attentive listening.

We also realize one characteristic difference between cortical networks built upon hemodynamic signals as compared to those derived from source-reconstructed narrow-band EEG signals. In the latter case, frequency-specific cortical networks did not exhibit modular organization (Figure S3). We note that cortical activities are organized across distributed neural processing streams and frequency channels which are superimposed and low-pass-filtered when imaged by fMRI (Logothetis et al., 2001; Heeger and Ress, 2002; Logothetis, 2008). Accordingly, frequency-resolved connectivity estimation would map spectrally and spatially distinct networks depending on the neurophysiological imaging technique, e.g. electrocorticography (He et al., 2008; Schölvinck et al., 2010; Kucyi et al., 2018) or E/MEG (Scheeringa et al., 2011; Liu et al., 2014; Siems et al., 2016). When estimation of connectivity as such is solely based on power-envelope correlations between alpha/beta oscillations in source-reconstructed E/MEG, the resulting network would be restricted to a fewer cortical regions and functional connections (Laufs et al., 2003; Brookes et al., 2011; Hipp and Siegel, 2015; Tewarie et al., 2016). Moreover, the spatial resolution with which these regions can be distinguished from one another is limited by the E/MEG sensor configuration (Farahibozorg et al., 2018). Indeed, in our data (source-reconstructed 64-channel EEG) anterior and medial-frontal cortical regions showed sparse connectivity (Figure 3). Thus, studying modular organization of large-scale neurophysiological networks would require the investigation of neural source activity over a broad frequency range with higher spatial resolution than EEG (see (Arnulfo et al., 2020) for a recent evidence).

Attentional modulation of neural responses within auditory cortex has been extensively investigated along different lines of research in auditory neuroscience (cf. Tune et al., 2020, for a study on auditory alpha power and neural tracking of speech using the same data and cohort as here). Nevertheless, large-scale network dynamic of the auditory brain has remained underexplored, particularly on the neurophysiological level. This is mainly due to the methodological challenges inherent to connectivity analysis (Schoffelen and Gross, 2009; O'Neill et al., 2015; Palva et al., 2018). In our methodology we carefully took these considerations into account. This eventually allowed us to functionally map and characterize large-scale neural connectivity within alpha and low-beta frequency channels whereby distant cortical nodes tuned into attentive listening under top-down control. Importantly, our brain-behavior findings add to the limited understanding of individual differences with which listeners cope with difficult listening situations. Looking ahead, this study opens new opportunities for brain network-based assessment of the hearing impaired as well as design of neurocognitive training strategies or assistive devices to rehabilitate or aid hearing.

Conclusion

In sum, the present study suggests that successful adaptation to a listening challenge latches onto two distinct yet complementary neural systems: beta-tuned frontoparietal network enabling the adaptation to the attentive listening state per se, and alpha-tuned posterior cortical network supporting attention to speech. Critically, connectivity dynamics of both networks appear under top-down control, and they predict individual differences in listening behavior. To conclude, we suggest that large-scale connectivity dynamics of intrinsic alpha and low-beta neural oscillations are closely linked to the control of auditory attention.

Materials and Methods

Data collection

This experiment was conducted as part of an ongoing large-scale study on the neural and cognitive mechanisms supporting adaptive listening behavior in healthy middle-aged and older adults ("The listening challenge: How ageing brains adapt (AUDADAPT)" https://cordis.europa.eu/project/id/646696). This project encompasses the collection of different demographic, behavioral, and neurophysiological measures across two time points. The analyses carried out on the data aim at relating adaptive listening behavior to changes in different neural dynamics (Alavash et al., 2019; Tune et al., 2020); see also https://osf.io/28r57/).

Participants and procedure

A total of N = 154 right-handed German native speakers (age range = 39–80 yrs, median age = 61 yrs, 62 males) participated in the study. All participants had normal or corrected-to-normal vision, did not report any neurological, psychiatric, or other disorders and were screened for mild cognitive impairment using the German version of the 6-Item Cognitive Impairment Test (6CIT; Jefferies and Gale, 2013). During EEG sessions participants first underwent 5-min eyes-open and 5-min eyes-closed resting-state measurements. The participants were asked not to think about something specific and to avoid movement during the measurements. Next, following task instruction, participants performed six blocks of a demanding dichotic listening task (Figure 1; see SI Appendix for details). As part of our large-scale study, prior to the EEG session participants also underwent a session consisting of a general screening procedure, detailed audiometric measurements, and a battery of cognitive tests and personality profiling (see Tune et al., 2018, for details). Only participants with normal hearing or age-adequate mild-to-moderate hearing loss were included in the present study. As part of this screening procedure, an additional 17 participants were excluded prior to EEG recording due to non-age-related hearing loss or a medical history. Three participants dropped out of the study prior to EEG recording and an additional 10 participants were excluded from analyses after EEG recording: three due to incidental findings after structural MR acquisition, six due to technical problems during EEG recording or overall poor EEG data quality, and one with four task-blocks only. Participants gave written informed consent and received financial compensation (8€ per hour). Procedures were approved by the ethics committee of the University of Lübeck and were in accordance with the Declaration of Helsinki.

EEG data analysis

Preprocessing. The artefact-clean continuous EEG data (see SI Appendix for details on EEG data acquisition and artefact rejection) were high-pass-filtered at 0.3 Hz (finite impulse response (FIR) filter, zero-phase lag, order 5574, Hann window) and low-pass-filtered at 180 Hz (FIR filter, zero-phase lag, order 100, Hamming window). Task data were cut into 10-s trials within –2 to 8 s relative to the

onset of the spatial-attention cue to capture cue presentation as well as the entire auditory stimulation interval. Resting-state data were similarly cut into 10-s epochs. Data were downsampled to f_s = 250 Hz. These procedures were implemented using Fieldtrip toolbox (Oostenveld et al., 2011).

Time-frequency analysis. Spectro-temporal estimates of single-trial task data were obtained for a time window of −1 to 7.5 s (relative to the onset of the spatial-attention cue) at frequencies ranging from 2 to 32 Hz on a logarithmic scale (Morlet's wavelets; number of cycles = 6, Fieldtrip implementation). The results were used for analyzing power modulation of brain oscillatory responses on sensor- and source-level (Figure S7). As a measure of nodal power, we used the mean of trial-average baseline-corrected source power within each time-frequency window of interest. The same time-frequency analysis was used for estimating power-envelope correlations during rest and task (see below).

Source projection of sensor data. Following EEG source and forward model construction (see SI Appendix for details) sensor-level single-trial (epoch) complex-value time-frequency estimates were projected to source space by matrix-multiplication of the common spatial filter weights (Figure S1B). To increase signal-to-noise ratio and computationally facilitate connectivity analyses, individual source-projected data were averaged across cortical surface grid-points per cortical patch defined according to the HCP functional parcellation template (Glasser et al., 2016; similar to Keitel and Gross, 2016). This parcellation provides a symmetrical delineation of each hemisphere into 180 parcels. This gave single-trial (or single-epoch) time-frequency source estimates at each cortical node. We note that a cortical parcellation with 360 nodes over-sample the realistic spatial resolution of 64-channel EEG. However, an optimal EEG-based cortical parcellation is currently not available, although studies have begun to fill this gap (Farahibozorg et al., 2018). Therefore, we used an established fMRI-based parcellation to approximate spatial boundaries of frequency-specific EEG source connectivity and its modulation throughout the listening task. This also allowed us to investigate the similarities and differences between fMRI and EEG whole-brain connectivity during rest and the same listening task in a subgroup of participants.

Connectivity analysis. Frequency-resolved connectivity analysis was done in the following steps per individual (see Figure S1B). First, trial-wise time-frequency source estimates were concatenated across time per frequency. For estimating resting-state connectivity this was done based on 5-min epoched data. For estimating overall connectivity during listening task irrespective of trial intervals (Figure 3), this was done by selecting 30 random trials per task block (equivalently, 5-min data). Then, connectivity matrices were averaged across six task blocks. This procedure assured that rest and task connectivity did not artificially differ due to differences in the duration of data used for estimating connectivity (van Diessen et al., 2015). For estimating task connectivity during each one-second time window (e.g., spatial-cue or final-word period; Figure 1, colored intervals) windowed signals were concatenated across all 240 trials (equivalently, 4-min data). Event-related task connectivity obtained from this procedure was then compared with 4-min resting state connectivity. To investigate the effect of block on connectivity (see Statistical analysis below), the same procedure was repeated based on all 40 trials per block. For this latter analysis, resting state connectivity was estimated based on 40 s of data. Thus, in all analyses data were matched in duration across rest, task, and all participants before estimation of connectivity.

Power-envelope correlation analysis. To assess frequency-specific neural interactions, we computed Pearson's correlations between the log-transformed power of all pairs of nodes (all-to-all connectivity). To eliminate the trivial common covariation in power measured from the same sources, we used the orthogonalization approach proposed by (Hipp et al., 2012) prior to computing the power correlations (Fieldtrip implementation). This approach has been suggested and used to

circumvent overestimation of instantaneous short-distance correlations, which can otherwise occur due to field propagation (Mehrkanoon et al., 2014; Colclough et al., 2015; Siems et al., 2016). The above procedure yielded frequency-specific 360-by-360 functional connectivity matrices per participant and carrier frequency (and trial interval). The between-subject reliability analysis (Figure S2; see SI Appendix for details) suggested that power-envelope correlations were strongest and showed highest reliability with 7-24 Hz. Accordingly, we focused our main analysis on three frequency bands within alpha and low-beta frequency range. Connectivity matrices in each frequency band was derived by averaging corresponding frequency-specific connectivity matrices. Change in connectivity was evaluated by first calculating task-connectivity matrix minus rest-connectivity matrix per frequency, and then averaging the results within each frequency band. Finally, connectivity matrices were thresholded at 10% of network density (proportional thresholding) (van Diessen et al., 2015). This procedure ensured that networks were matched in density across rest, task, and all participants. Subsequently, nodal connectivity was obtained by calculating the sum of each node's connection weights (i.e., correlations values). Mean connectivity of a network (e.g., the frontoparietal network) was obtained by averaging nodal connectivity values across the network.

Statistical analysis

Behavioral data. Participants' behavioral performance in the listening task was evaluated with respect to accuracy and response speed. Trials in which participants failed to answer within the given 4-s response window ('timeouts') were excluded from the analysis. Spatial stream confusions, that is trials in which the final word of the to-be-ignored speech stream were selected, and random errors were jointly classified as incorrect answers. The analysis of response speed, defined as the inverse of reaction time, was based on correct trials only.

Connectivity data. Statistical comparisons of nodal and mean connectivity between rest and task were based on permutation tests for paired samples (randomly permuting the rest and task labels 10,000 times). We used Cohen's d for paired samples as the corresponding effect size. For nodal connectivity analysis, and to correct for multiple comparisons entailed by the neumebr of cortical nodes, we used FDR procedure at significance level of 0.01 (two-sided). Knowing the skewed distribution of mean connectivity, these valuse were logit-transformed before submitting to (generalized) linear mixed-effects models (see below).

Brain-behavior models. Brain-behavior relationship was investigated within a linear mixed-effects analysis framework. To this end, either of the single-trial behavioral measures (accuracy or response speed) across all participants were treated as the dependent variable. The main experimental predictors in the model were the single-trial spatial and semantic cue conditions, each at two levels (divided vs. selective and general vs. specific, respectively). Neural predictors entered as between-subject regressors. These include mean resting state connectivity, mean event-related task connectivity per block, and mean event-related neural oscillatory power (dB) per block. The linear mixed-effects analysis framework allowed us to account for other variables which entered as regressors of no-interest in the model. These include age, mean pure-tone audiometry (PTA) averaged across left and right ear, side probed (left or right), and task-block number. Mixed-effects analyses were implemented in R (R Core Team, 2017) using the packages lme4 (Bates et al., 2015), effects (Fox and Weisberg, 2018) and sjPlot (https://strengejacke.github.io/sjPlot/).

Model estimation. The regressors in each brain-behavior model included the main effects of all predictors introduced above, plus the interaction between the two listening cues and the interaction between rest and task connectivity. Additional interaction terms were also included to explore their

possible effects on listening behavior. The influence of listening cues and of neural measures were tested in same brain-behavior model. The models also included random intercepts by subject. In a data-driven manner, we then tested whether model fit (performed using maximum-likelihood estimation) could be further improved by the inclusion of subject-specific random slopes for the effects of the spatial-attention cue, semantic cue, or probed ear. The change in model fit was assessed using likelihood ratio tests on nested models. Deviation coding was used for categorical predictors. All continuous variables were z-scored. For the dependent measure of accuracy, we used generalized linear mixed-effects model (binomial distribution, logit link function). For response speed, we used general linear mixed-effects model (gaussian distribution, identity link function). Given the large sample size, p-values for individual model terms are based on Wald t-as z-values for linear models (Luke, 2017) and on z-values and asymptotic Wald tests in generalized linear models. All reported p-values are corrected to control for the false discovery rate. As a measure of effects size, for the model predicting accuracy we report odds ratios (OR) and for response speed we report the regression coefficient (β).

Bayes factor. To facilitate the interpretability of significant and non-significant effects, we calculated the Bayes Factor (BF) based on the comparison of Bayesian information criterion (BIC) values as proposed by (Wagenmakers, 2007) : BF = exp([BIC(H0)–BIC(H1)]/2). To calculate the BF for a given term, we compared the BIC values of the full model to that of a reduced model in which only the rest-connectivity × task-connectivity interaction term was removed. By convention, log-BFs larger than 1 provide evidence for the presence of an effect (i.e., the observed data are more likely under the more complex model) whereas log-BFs smaller than −1 provide evidence for the absence of an effect (i.e., the observed data are more likely under the simpler model) (Dienes, 2014).

Data visualization

Brain surfaces were visualized using the Connectome Workbench. Brain-behavior interaction plots were visualize using R package effects (Fox and Weisberg, 2018).

Data availability

In accordance with recommendations for best practices in data analysis and sharing (Pernet et al., 2019; Pernet et al., 2020) the complete dataset associated with this work will be publicly available under https://osf.io/28r57/

Acknowledgement

Research was supported by the European Research Council (ERC Consolidator grant AUDADAPT, no. 646696 to JO) and German Research Foundation (DFG grant, no. AL2408/1-1 to MA). Parts of the connectivity analyses were conducted using the OMICS compute cluster at the University of Lübeck. The authors are grateful for the help of Franziska Scharata in acquiring the data.

References

Alavash M, Tune S, Obleser J (2019) Modular reconfiguration of an auditory control brain network supports adaptive listening behavior. Proceedings of the National Academy of Sciences of the United States of America 116:660-669.

Antzoulatos EG, Miller EK (2016) Synchronous beta rhythms of frontoparietal networks support only behaviorally relevant representations. Elife 5.

Arnulfo G, Wang SH, Myrov V, Toselli B, Hirvonen J, Fato MM, Nobili L, Cardinale F, Rubino A, Zhigalov A, Palva S, Palva JM (2020) Long-range phase synchronization of high-frequency oscillations in human cortex. Nat Commun 11:5363.

Banerjee S, Snyder AC, Molholm S, Foxe JJ (2011) Oscillatory alpha-band mechanisms and the deployment of spatial attention to anticipated auditory and visual target locations: supramodal or sensory-specific control mechanisms? The Journal of neuroscience : the official journal of the Society for Neuroscience 31:9923-9932.

Bastos AM, Usrey WM, Adams RA, Mangun GR, Fries P, Friston KJ (2012) Canonical microcircuits for predictive coding. Neuron 76:695-711.

Bastos AM, Vezoli J, Bosman CA, Schoffelen JM, Oostenveld R, Dowdall JR, De Weerd P, Kennedy H, Fries P (2015) Visual areas exert feedforward and feedback influences through distinct frequency channels. Neuron 85:390-401.

Bates D, Mächler M, Bolker B, Walker S (2015) Fitting linear mixed-effects models using lme4. Journal of Statistical Software 67.

Billig AJ, Herrmann B, Rhone AE, Gander PE, Nourski KV, Snoad BF, Kovach CK, Kawasaki H, Howard MA, 3rd, Johnsrude IS (2019) A Sound-Sensitive Source of Alpha Oscillations in Human Non-Primary Auditory Cortex. The Journal of neuroscience : the official journal of the Society for Neuroscience 39:8679-8689.

Bonnefond M, Kastner S, Jensen O (2017) Communication between Brain Areas Based on Nested Oscillations. eNeuro 4.

Broadbent DE, Gregory M (1964) Accuracy of recognition for speech presented to the right and left ears. Quarterly Journal of Experimental Psychology 16:359-360.

Brookes MJ, Woolrich M, Luckhoo H, Price D, Hale JR, Stephenson MC, Barnes GR, Smith SM, Morris PG (2011) Investigating the electrophysiological basis of resting state networks using magnetoencephalography. Proceedings of the National Academy of Sciences of the United States of America 108:16783-16788.

Buschman TJ, Denovellis EL, Diogo C, Bullock D, Miller EK (2012) Synchronous oscillatory neural ensembles for rules in the prefrontal cortex. Neuron 76:838-846.

Capotosto P, Babiloni C, Romani GL, Corbetta M (2009) Frontoparietal cortex controls spatial attention through modulation of anticipatory alpha rhythms. The Journal of neuroscience : the official journal of the Society for Neuroscience 29:5863-5872.

Clayton MS, Yeung N, Cohen Kadosh R (2018) The many characters of visual alpha oscillations. Eur J Neurosci 48:2498-2508.

Colclough GL, Brookes MJ, Smith SM, Woolrich MW (2015) A symmetric multivariate leakage correction for MEG connectomes. NeuroImage 117:439-448.

D'Andrea A, Chella F, Marshall TR, Pizzella V, Romani GL, Jensen O, Marzetti L (2018) Alpha and alpha-beta phase synchronization mediate the recruitment of the visuospatial attention network through the Superior Longitudinal Fasciculus. NeuroImage 188:722-732.

Dai L, Best V, Shinn-Cunningham BG (2018) Sensorineural hearing loss degrades behavioral and physiological measures of human spatial selective auditory attention. Proceedings of the National Academy of Sciences of the United States of America 115:E3286-E3295.

de Pesters A, Coon WG, Brunner P, Gunduz A, Ritaccio AL, Brunet NM, de Weerd P, Roberts MJ, Oostenveld R, Fries P, Schalk G (2016) Alpha power indexes task-related networks on large and small scales: A multimodal ECoG study in humans and a non-human primate. NeuroImage 134:122-131.

Deal JA, Betz J, Yaffe K, Harris T, Purchase-Helzner E, Satterfield S, Pratt S, Govil N, Simonsick EM, Lin FR, Health ABCSG (2017) Hearing Impairment and Incident Dementia and Cognitive Decline in Older Adults: The Health ABC Study. J Gerontol A Biol Sci Med Sci 72:703-709.

Dienes Z (2014) Using Bayes to get the most out of non-significant results. Front Psychol 5:781.

Engel AK, Fries P (2010) Beta-band oscillations--signalling the status quo? Current opinion in neurobiology 20:156-165.

Engel AK, Gerloff C, Hilgetag CC, Nolte G (2013) Intrinsic coupling modes: multiscale interactions in ongoing brain activity. Neuron 80:867-886.

Farahibozorg SR, Henson RN, Hauk O (2018) Adaptive cortical parcellations for source reconstructed EEG/MEG connectomes. NeuroImage 169:23-45.

Fiebelkorn IC, Kastner S (2020) Functional Specialization in the Attention Network. Annu Rev Psychol 71:221-249.

Fox J, Weisberg S (2018) Visualizing Fit and Lack of Fit in Complex Regression Models with Predictor Effect Plots and Partial Residuals. Journal of Statistical Software 87.

Foxe JJ, Snyder AC (2011) The Role of Alpha-Band Brain Oscillations as a Sensory Suppression Mechanism during Selective Attention. Front Psychol 2:154.

Fusi S, Miller EK, Rigotti M (2016) Why neurons mix: high dimensionality for higher cognition. Current opinion in neurobiology 37:66-74.

Glasser MF, Coalson TS, Robinson EC, Hacker CD, Harwell J, Yacoub E, Ugurbil K, Andersson J, Beckmann CF, Jenkinson M, Smith SM, Van Essen DC (2016) A multi-modal parcellation of human cerebral cortex. Nature 536:171-178.

Haegens S, Nacher V, Luna R, Romo R, Jensen O (2011) alpha-Oscillations in the monkey sensorimotor network influence discrimination performance by rhythmical inhibition of neuronal spiking. Proceedings of the National Academy of Sciences of the United States of America 108:19377-19382.

He BJ, Snyder AZ, Zempel JM, Smyth MD, Raichle ME (2008) Electrophysiological correlates of the brain's intrinsic large-scale functional architecture. Proceedings of the National Academy of Sciences of the United States of America 105:16039-16044.

Heeger DJ, Ress D (2002) What does fMRI tell us about neuronal activity? Nature reviews Neuroscience 3:142-151.

Hipp JF, Siegel M (2015) BOLD fMRI Correlation Reflects Frequency-Specific Neuronal Correlation. Current biology : CB 25:1368-1374.

Hipp JF, Hawellek DJ, Corbetta M, Siegel M, Engel AK (2012) Large-scale cortical correlation structure of spontaneous oscillatory activity. Nature neuroscience 15:884-890.

Jefferies K, Gale TM (2013) Six-Item Cognitive Impairment Test (6CIT). . in Cognitive Screening Instruments (Springer, 1109 London, 2013):209-218.

Jensen O, Mazaheri A (2010) Shaping functional architecture by oscillatory alpha activity: gating by inhibition. Frontiers in human neuroscience 4:186.

Jensen O, Gips B, Bergmann TO, Bonnefond M (2014) Temporal coding organized by coupled alpha and gamma oscillations prioritize visual processing. Trends Neurosci 37:357-369.

Keitel A, Gross J (2016) Individual human brain areas can be identified from their characteristic spectral activation fingerprints. PLOS Biology 14:e1002498.

Kelly SP, O'Connell RG (2015) The neural processes underlying perceptual decision making in humans: recent progress and future directions. J Physiol Paris 109:27-37.

Kimura D (1961) Cerebral dominance and the perception of verbal stimuli. Canadian Journal of Psychology/Revue canadienne de psychologie 15:166-171.

Klimesch W, Sauseng P, Hanslmayr S (2007) EEG alpha oscillations: the inhibition-timing hypothesis. Brain Res Rev 53:63-88.

Kopell N, Whittington MA, Kramer MA (2011) Neuronal assembly dynamics in the beta1 frequency range permits short-term memory. Proceedings of the National Academy of Sciences of the United States of America 108:3779-3784.

Kucyi A, Schrouff J, Bickel S, Foster BL, Shine JM, Parvizi J (2018) Intracranial Electrophysiology Reveals Reproducible Intrinsic Functional Connectivity within Human Brain Networks. The Journal of neuroscience : the official journal of the Society for Neuroscience 38:4230-4242.

Laufs H, Krakow K, Sterzer P, Eger E, Beyerle A, Salek-Haddadi A, Kleinschmidt A (2003) Electroencephalographic signatures of attentional and cognitive default modes in spontaneous brain activity fluctuations at rest. Proceedings of the National Academy of Sciences of the United States of America 100:11053-11058.

Lee JH, Whittington MA, Kopell NJ (2013) Top-down beta rhythms support selective attention via interlaminar interaction: a model. PLoS Comput Biol 9:e1003164.

Lin FR, Yaffe K, Xia J, Xue QL, Harris TB, Purchase-Helzner E, Satterfield S, Ayonayon HN, Ferrucci L, Simonsick EM, Health ABCSG (2013) Hearing loss and cognitive decline in older adults. JAMA Intern Med 173:293-299.

Liu Z, de Zwart JA, Chang C, Duan Q, van Gelderen P, Duyn JH (2014) Neuroelectrical decomposition of spontaneous brain activity measured with functional magnetic resonance imaging. Cereb Cortex 24:3080-3089.

Logothetis NK (2008) What we can do and what we cannot do with fMRI. Nature 453:869-878.

Logothetis NK, Pauls J, Augath M, Trinath T, Oeltermann A (2001) Neurophysiological investigation of the basis of the fMRI signal. Nature 412:150-157.

Luke SG (2017) Evaluating significance in linear mixed-effects models in R. Behav Res Methods 49:1494-1502.

Mantini D, Perrucci MG, Del Gratta C, Romani GL, Corbetta M (2007) Electrophysiological signatures of resting state networks in the human brain. Proceedings of the National Academy of Sciences of the United States of America 104:13170-13175.

Marshall TR, Bergmann TO, Jensen O (2015a) Frontoparietal Structural Connectivity Mediates the Top-Down Control of Neuronal Synchronization Associated with Selective Attention. PLoS Biol 13:e1002272.

Marshall TR, O'Shea J, Jensen O, Bergmann TO (2015b) Frontal eye fields control attentional modulation of alpha and gamma oscillations in contralateral occipitoparietal cortex. The Journal of neuroscience : the official journal of the Society for Neuroscience 35:1638-1647.

Mathewson KE, Lleras A, Beck DM, Fabiani M, Ro T, Gratton G (2011) Pulsed out of awareness: EEG alpha oscillations represent a pulsed-inhibition of ongoing cortical processing. Front Psychol 2:99.

Mattys SL, Davis MH, Bradlow AR, Scott SK (2012) Speech recognition in adverse conditions: A review. Language and Cognitive Processes 27:953-978.

Mehrkanoon S, Breakspear M, Britz J, Boonstra TW (2014) Intrinsic coupling modes in source-reconstructed electroencephalography. Brain Connectivity 4:812-825.

Miller EK, Buschman TJ (2013) Cortical circuits for the control of attention. Current opinion in neurobiology 23:216-222.

Miller EK, Lundqvist M, Bastos AM (2018) Working Memory 2.0. Neuron 100:463-475.

Müller N, Weisz N (2012) Lateralized auditory cortical alpha band activity and interregional connectivity pattern reflect anticipation of target sounds. Cereb Cortex 22:1604-1613.

O'Neill GC, Barratt EL, Hunt BA, Tewarie PK, Brookes MJ (2015) Measuring electrophysiological connectivity by power envelope correlation: a technical review on MEG methods. Phys Med Biol 60:R271-295.

Oostenveld R, Fries P, Maris E, Schoffelen JM (2011) FieldTrip: Open source software for advanced analysis of MEG, EEG, and invasive electrophysiological data. Computational intelligence and neuroscience 2011:156869.

Palva JM, Wang SH, Palva S, Zhigalov A, Monto S, Brookes MJ, Schoffelen JM, Jerbi K (2018) Ghost interactions in MEG/EEG source space: A note of caution on inter-areal coupling measures. NeuroImage 173:632-643.

Palva S, Palva JM (2007) New vistas for alpha-frequency band oscillations. Trends Neurosci 30:150-158.

Palva S, Palva JM (2011) Functional roles of alpha-band phase synchronization in local and large-scale cortical networks. Front Psychol 2:204.

Palva S, Palva JM (2012) Discovering oscillatory interaction networks with M/EEG: challenges and breakthroughs. Trends in cognitive sciences 16:219-230.

Peelle JE (2017) Listening Effort: How the Cognitive Consequences of Acoustic Challenge Are Reflected in Brain and Behavior. Ear Hear.

Pernet C, Garrido MI, Gramfort A, Maurits N, Michel CM, Pang E, Salmelin R, Schoffelen JM, Valdes-Sosa PA, Puce A (2020) Issues and recommendations from the OHBM COBIDAS MEEG committee for reproducible EEG and MEG research. Nature neuroscience 23:1473-1483.

Pernet CR, Appelhoff S, Gorgolewski KJ, Flandin G, Phillips C, Delorme A, Oostenveld R (2019) EEG-BIDS, an extension to the brain imaging data structure for electroencephalography. Scientific Data 6.

Pesaran B, Vinck M, Einevoll GT, Sirota A, Fries P, Siegel M, Truccolo W, Schroeder CE, Srinivasan R (2018) Investigating large-scale brain dynamics using field potential recordings: analysis and interpretation. Nature neuroscience 21:903-919.

Popov T, Kastner S, Jensen O (2017) FEF-Controlled Alpha Delay Activity Precedes Stimulus-Induced Gamma-Band Activity in Visual Cortex. The Journal of neuroscience : the official journal of the Society for Neuroscience 37:4117-4127.

Rigotti M, Barak O, Warden MR, Wang XJ, Daw ND, Miller EK, Fusi S (2013) The importance of mixed selectivity in complex cognitive tasks. Nature 497:585-590.

Sadaghiani S, Kleinschmidt A (2016) Brain Networks and alpha-Oscillations: Structural and Functional Foundations of Cognitive Control. Trends in cognitive sciences 20:805-817.

Sadaghiani S, Scheeringa R, Lehongre K, Morillon B, Giraud AL, Kleinschmidt A (2010) Intrinsic connectivity networks, alpha oscillations, and tonic alertness: a simultaneous electroencephalography/functional magnetic resonance imaging study. The Journal of neuroscience : the official journal of the Society for Neuroscience 30:10243-10250.

Sadaghiani S, Scheeringa R, Lehongre K, Morillon B, Giraud AL, D'Esposito M, Kleinschmidt A (2012) alpha-band phase synchrony is related to activity in the fronto-parietal adaptive control network. The Journal of neuroscience : the official journal of the Society for Neuroscience 32:14305-14310.

Sadaghiani S, Dombert PL, Lovstad M, Funderud I, Meling TR, Endestad T, Knight RT, Solbakk AK, D'Esposito M (2018) Lesions to the Fronto-Parietal Network Impact Alpha-Band Phase Synchrony and Cognitive Control. Cereb Cortex.

Salazar R, Dotson N, Bressler S, Gray C (2012) Contentspecific fronto-parietal synchronization during visual working memory. Science:1097–1100.

Scheeringa R, Fries P, Petersson KM, Oostenveld R, Grothe I, Norris DG, Hagoort P, Bastiaansen MC (2011) Neuronal dynamics underlying high- and low-frequency EEG oscillations contribute independently to the human BOLD signal. Neuron 69:572-583.

Schoffelen JM, Gross J (2009) Source connectivity analysis with MEG and EEG. Human brain mapping 30:1857-1865.

Schölvinck M, Maier A, Ye F, Duyn J, Leopold D (2010) Neural basis of global resting-state fMRI activity. PNAS 107:10238-10243.

Shinn-Cunningham B (2017) Cortical and Sensory Causes of Individual Differences in Selective Attention Ability Among Listeners With Normal Hearing Thresholds. J Speech Lang Hear Res 60:2976-2988.

Shinn-Cunningham BG, Best V (2008) Selective Attention in Normal and Impaired Hearing. Trends Amplif 12:283-299.

Siegel M, Engel AK, Donner TH (2011) Cortical network dynamics of perceptual decision-making in the human brain. Frontiers in human neuroscience 5:21.

Siegel M, Donner TH, Engel AK (2012) Spectral fingerprints of large-scale neuronal interactions. Nature reviews Neuroscience 13:121-134.

Siegel M, Buschman TJ, Miller EK (2015) Cortical information flow during flexible sensorimotor decisions. 348.

Siems M, Pape AA, Hipp JF, Siegel M (2016) Measuring the cortical correlation structure of spontaneous oscillatory activity with EEG and MEG. NeuroImage 129:345-355.

Spitzer B, Blankenburg F (2011) Stimulus-dependent EEG activity reflects internal updating of tactile working memory in humans. Proceedings of the National Academy of Sciences of the United States of America 108:8444–8449.

Spitzer B, Haegens S (2017) Beyond the Status Quo: A Role for Beta Oscillations in Endogenous Content (Re-) Activation. eneuro:ENEURO.0170-0117.2017.

Spitzer B, Fleck S, Blankenburg F (2014) Parametric alpha- and beta-band signatures of supramodal numerosity information in human working memory. The Journal of neuroscience : the official journal of the Society for Neuroscience 34:4293-4302.

Stanley DA, Roy JE, Aoi MC, Kopell NJ, Miller EK (2016) Low-Beta oscillations turn up the gain during category judgments. Cerebral Cortex:1-15.

Tamati TN, Gilbert JL, Pisoni DB (2013) Some factors underlying individual differences in speech recognition on PRESTO: a first report. J Am Acad Audiol 24:616-634.

Tewarie P, Bright MG, Hillebrand A, Robson SE, Gascoyne LE, Morris PG, Meier J, Van Mieghem P, Brookes MJ (2016) Predicting haemodynamic networks using electrophysiology: The role of non-linear and cross-frequency interactions. NeuroImage 130:273-292.

Tewarie P, Hunt BAE, O'Neill GC, Byrne A, Aquino K, Bauer M, Mullinger KJ, Coombes S, Brookes MJ (2018) Relationships Between Neuronal Oscillatory Amplitude and Dynamic Functional Connectivity. Cereb Cortex.

Tune S, Wostmann M, Obleser J (2018) Probing the limits of alpha power lateralisation as a neural marker of selective attention in middle-aged and older listeners. Eur J Neurosci 48:2537-2550.

Tune S, Alavash M, Fiedler L, Obleser J (2020) The impact of neural attentional filters on listening behavior in a large cohort of aging individuals. BioRxiv.

Van Diepen RM, Foxe JJ, Mazaheri A (2019) The functional role of alpha-band activity in attentional processing: the current zeitgeist and future outlook. Curr Opin Psychol 29:229-238.

van Diessen E, Numan T, van Dellen E, van der Kooi AW, Boersma M, Hofman D, van Lutterveld R, van Dijk BW, van Straaten EC, Hillebrand A, Stam CJ (2015) Opportunities and methodological challenges in EEG and MEG resting state functional brain network research. Clinical neurophysiology : official journal of the International Federation of Clinical Neurophysiology 126:1468-1481.

Wagenmakers EJ (2007) A practical solution to the pervasive problems of p values. Psychonomic Bulletin & Review 14:779-804.

Weisz N, Muller N, Jatzev S, Bertrand O (2014) Oscillatory alpha modulations in right auditory regions reflect the validity of acoustic cues in an auditory spatial attention task. Cereb Cortex 24:2579-2590.

Wimmer K, Ramon M, Pasternak T, Compte A (2016) Transitions between Multiband Oscillatory Patterns Characterize Memory-Guided Perceptual Decisions in Prefrontal Circuits. The Journal of neuroscience : the official journal of the Society for Neuroscience 36:489-505.

Wöstmann M, Alavash M, Obleser J (2019) Alpha Oscillations in the Human Brain Implement Distractor Suppression Independent of Target Selection. The Journal of neuroscience : the official journal of the Society for Neuroscience 39:9797-9805.

Wöstmann M, Herrmann B, Maess B, Obleser J (2016) Spatiotemporal dynamics of auditory attention synchronize with speech. Proceedings of the National Academy of Sciences of the United States of America 113:3873–3878.